



# Characterization of a high light yield liquid scintillator with a novel organosilicon fluor developed for astroparticle physics experiments

A. Sidorenkov<sup>1,a</sup>, O. Borshchev<sup>2,3</sup>, A. Fazliakhmetov<sup>1</sup>, A. Lukanov<sup>1</sup>, B. Lubsandorzhiev<sup>1</sup>, S. Lubsandorzhiev<sup>1</sup>, D. Nanzanov<sup>1</sup>, S. Ponomarenko<sup>2</sup>, M. Skorotetcky<sup>2</sup>, N. Surin<sup>2</sup>, E. Svidchenko<sup>2</sup>, N. Ushakov<sup>1</sup>, D. Voronin<sup>1</sup>

<sup>1</sup> Institute for Nuclear Research of the Russian Academy of Sciences, pr-t 60-letiya Oktyabrya 7a, Moscow 117312, Russian Federation

<sup>2</sup> Enikolopov Institute of Synthetic Polymeric Materials of the Russian Academy of Sciences, ul. Profsoyuznaya 70, Moscow 117393, Russian Federation

<sup>3</sup> “LumInnoTech” LLC, ul. Profsoyuznaya 70, Moscow 117393, Russian Federation

Received: 17 June 2022 / Accepted: 7 November 2022  
© The Author(s) 2022

**Abstract** A new high light yield liquid scintillator based on linear alkylbenzene (LAB) as an organic solvent and a novel nanostructured organosilicon liminophore as a scintillation fluor has been developed for the next generation large-scale experiments in astroparticle physics. It is shown that the developed liquid scintillator has light yield almost two times higher than traditional LAB-based liquid scintillator with PPO fluor, when peak light yield values are compared, since the former peaks at 490 nm, while the latter peaks at 360 nm. At the same time light emission kinetics is characterized by about 10 ns decay time constant for its fastest component which contributes more than 80% to the total light yield of the scintillator.

## 1 Introduction

Liquid scintillators have always been an important part of many experiments in neutrino physics. Today, great success has been achieved in carrying out precision measurements of the properties of neutrinos (antineutrinos) in experiments such as KamLAND [1], Borexino [2], Daya Bay [3], RENO [4], Double Chooz [5]. These experiments have successfully deployed large volumes of organic liquid scintillator to detect neutrinos with high efficiency. Presently the next-generation neutrino experiment JUNO with 20 kt liquid scintillator is being under construction in China [6].

A liquid organic scintillator is usually composed of a solvent and scintillation dopants (fluors): a primary fluor with a concentration of a few grams per litre of solvent

and a secondary wavelength shifting fluor with substantially lower concentration. Recently, linear alkylbenzene (LAB) is gaining popularity as a base solvent. Its advantages are low toxicity, high transparency, high flash point and relatively low cost. 2,5-Diphenyloxazole, also known as PPO, has been widely used as the primary fluor. 1,4-Bis(2-methylstyryl)benzene (bis-MSB) or 1,4-bis(5-phenyloxazol-2-yl)benzene (POPOP) are used as the second wavelength shifting fluor. The standard LAB-based liquid scintillator with the addition of PPO and bis-MSB or POPOP has been successfully applied in large-scale experiments such as Daya Bay [7] and RENO [8].

A new organosilicon fluor for a LAB-based liquid scintillator, so called NOL 37 (Nanostructured Organosilicon Luminophore 37) [9], is proposed and developed as an alternative to the “standard” composition of fluors (PPO + bis MSB or POPOP). A picture of samples of the LAB-based liquid scintillators with NOL 37 and PPO fluors is shown in Fig. 1. One of advantages of this fluor is that there is no need to use an additional wavelength shifting fluor anymore. In this paper, a liquid scintillator, consisting of LAB as a solvent and NOL 37 as a fluor has been extensively studied.

## 2 Absorbtion and emission spectra of the NOL 37

Molecules of the organosilicon fluor have donor and acceptor sites that can effectively produce scintillation light through the mechanism of Förster resonance energy transfer (FRET). The excitation energy is absorbed by a donor site of the molecule and transferred via silicon to an acceptor site,

<sup>a</sup> e-mail: andy-27@yandex.ru (corresponding author)

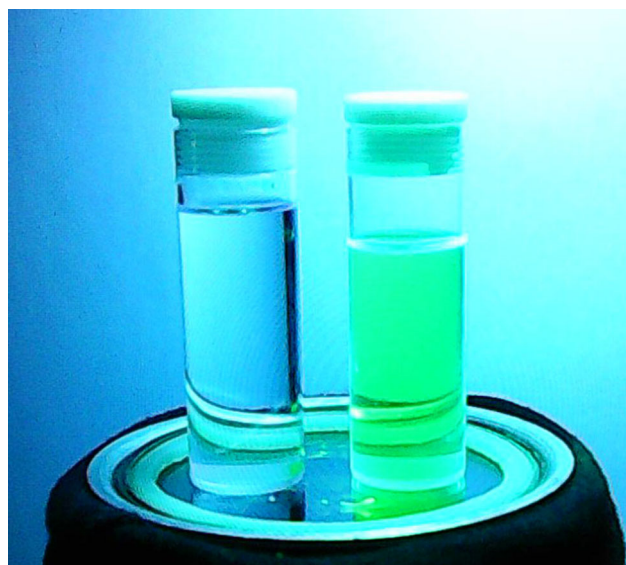


**Fig. 1** The sample of the LAB-based scintillator with NOL 37 (vial on the right) and “standard” scintillator with PPO (vial on the left)

which emits scintillation photons in response. This approach provides a high conversion efficiency of ionization energy into scintillation light with a high Stokes shift of about 100 nm compared to the standard approach when two fluors are used. Typical absorption and emission spectra of NOL 37 are shown in Fig. 2. The small overlap area of the absorption and emission spectra indicates that reabsorption is very small. Absorption and emission spectra measurements were performed using the scientific equipment of Research Sharing Center “Center for Polymer Research”, ISPM RAS.

The maximum of the emission spectrum of NOL 37 lies in the region of about 490–500 nm. Therefore, there is a mismatch of emission spectrum of NOL 37 and sensitivity curves of contemporary bialkali photocathodes usually used in photomultiplier tubes (PMTs). This problem has to be solved by adjusting the sensitivity of photomultiplier tubes to match the emission spectra of new scintillation fluors. One option is to use PMTs with a multialkali photocathode with their sensitivity maximum corresponding to the maximum of the emission spectrum of the new fluors.

The new fluor will also help to solve the problem of solvent purification, which is so critical for large-scale scintillator detectors. It is possible to use unpurified solvents because the emission spectrum with a maximum at about 490–500 nm lies in the region where the transparency of even “raw” unpurified solvents is high. This property is a great advantage, since there will be no need to create huge multistage purification systems.

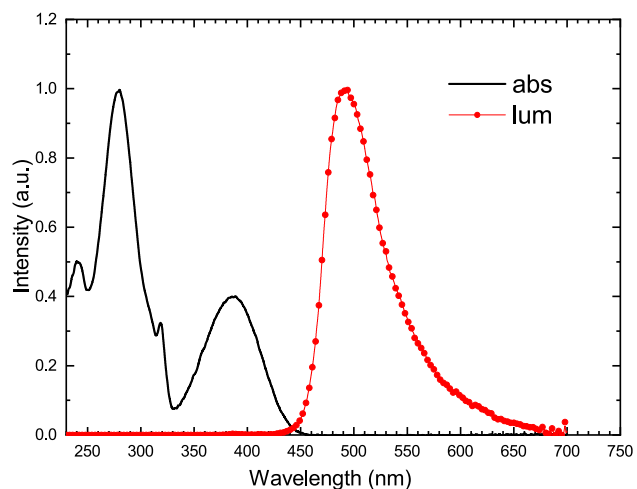


**Fig. 2** Typical absorption (black colour) and emission spectra (red colour) of the NOL 37 fluor

### 3 Light yield and emission kinetics measurements of LAB-based scintillator with NOL 37 fluor

The main properties of the LAB-based scintillator with NOL 37 fluor such as light yield and emission kinetics have been extensively characterized and studied. The measurements of the light yield and the emission kinetics were carried out using a specialized setup. The liquid scintillator mixtures were poured into a cylindrical quartz cuvette. The diameter and height of the cuvette are 20 mm and 10 mm respectively. The measurement of the light yield was performed by a Photonis XP5301B PMT with high quantum efficiency bialkali photocathode. The PMT signals are digitized by LeCroy 2249W charge-to-digital converter. The cuvette was irradiated by 662 keV gamma-quanta from a  $^{137}\text{Cs}$  radioactive source. Figure 3 shows the measured energy spectra of LAB-based scintillators with different concentrations of the NOL 37 fluor.

The light yield of the scintillators with NOL 37 fluor was evaluated by normalizing to the LAB-based scintillator with the addition of 1.5 g/L PPO. Due to the small size of the cuvette, there is no need to add a wavelength shifter to scintillator. The energy spectrum of LAB + 1.5 g/L PPO is also shown in Fig. 3. The position of the Compton edge and the corresponding charge were determined. The light yield values were obtained in arbitrary units.

The dependence of the PMT quantum efficiency on wavelength was measured carefully in our lab. The mean value of the PMT quantum efficiency averaged over emission spectra of PPO and NOL 37 in the wavelength range between 300 and 700 nm was calculated using the weighted arithmetic mean formula:

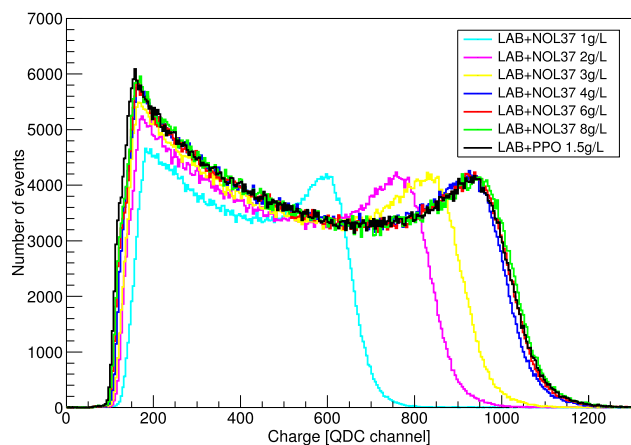


**Fig. 3** Results of light yield measurements of liquid scintillators with NOL 37 fluor under irradiation by 662 keV gamma-quanta from  $^{137}\text{Cs}$  radioactive source

$$\langle \eta \rangle = \frac{\sum_{\lambda=300}^{700} S_{\lambda} \cdot \eta_{\lambda}}{\sum_{\lambda=300}^{700} S_{\lambda}} \quad (1)$$

where  $S_{\lambda}$  is the intensity of the emission spectrum of the scintillation fluor for a given wavelength  $\lambda$ , and  $\eta_{\lambda}$  is the quantum efficiency of the PMT corresponding to this wavelength.

The PMT quantum efficiency vs wavelength curve and two emission spectra of PPO and NOL 37 are shown in Fig. 4.

The average quantum efficiency of the XP5301B is  $\langle \eta \rangle_{\text{PPO}} = 42.1\%$  and  $\langle \eta \rangle_{\text{NOL37}} = 19.1\%$  over the emission spectra of PPO and NOL 37 respectively.

In Fig. 5 the dependences of the light yield of LAB-based scintillator on the concentration of NOL 37 and PPO fluors are shown, taking into account the quantum efficiency of the XP5301B. The light yield of the scintillators with NOL 37 is almost two times higher than the light yield of the scintillator with PPO. The ratio of light yields  $LY_{\text{NOL37}}/LY_{\text{PPO}}$

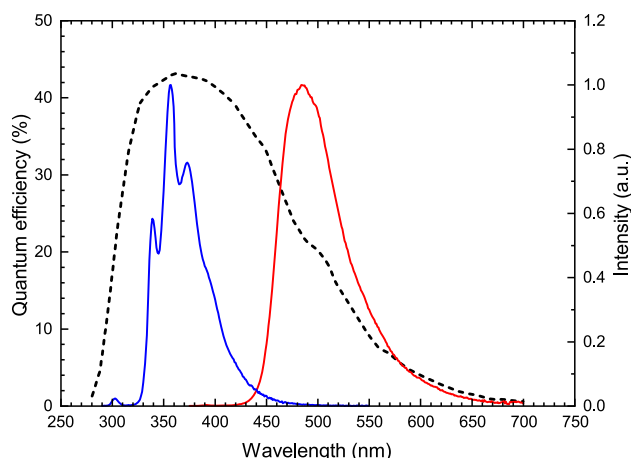


**Fig. 4** XP5301B quantum efficiency curve (black colour) and emission spectra of PPO (blue colour) and NOL 37 (red colour)

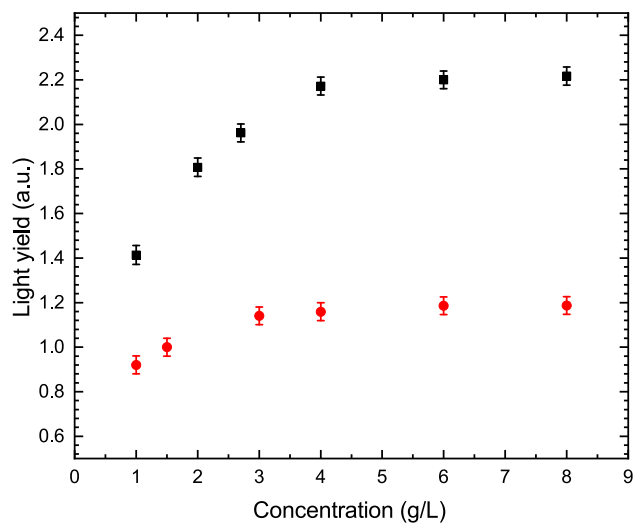


**Fig. 5** Dependence of the light yield on the concentration of the NOL 37 (black colour) and PPO (red colour) fluors

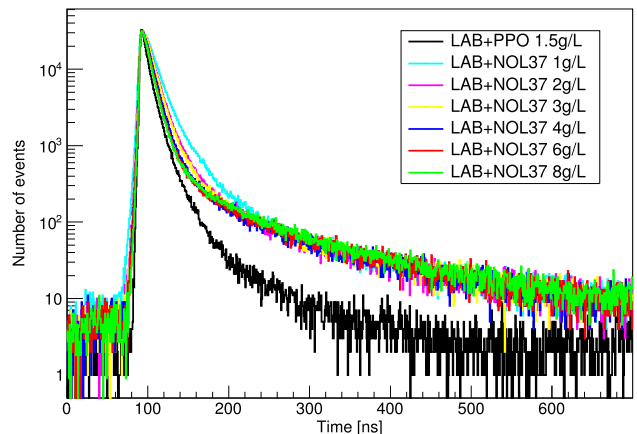


**Fig. 6** Light emission kinetics of liquid scintillators with NOL 37 fluors

was determined to be  $1.87 \pm 0.08$  at fluors concentrations of 4 g/L, where  $LY_{\text{NOL37}}$  and  $LY_{\text{PPO}}$  are light yields of liquid scintillators with NOL 37 and PPO respectively. Light yields of both liquid scintillators are already saturated at fluor concentration of 4 g/l.

The emission kinetics spectra were measured by a time correlated single-photon counting technique [10]. In this case, two fast PMTs (Hamamatsu R6427 and Photonis XP3112PA) and wide-range time-to-digital converter with a channel width of 75 ps were used to measure the emission kinetics. In Fig. 6 the spectra of the emission kinetics of LAB-based scintillators with NOL 37 and PPO fluors under irradiation by gamma-quanta from  $^{137}\text{Cs}$  radioactive source are shown.

The kinetics of the scintillation process in the LAB-based scintillators with new fluor has a complex multicomponent character. The scintillation pulse is characterized by three

**Table 1** Decay time constants of scintillation pulse of LAB-based scintillators with new fluors

Contents of NOL 37 (g/L)	Decay time constant (ns)		
	$\tau_1$	$\tau_2$	$\tau_3$
1	14.6 $\pm$ 0.6 (82%)	52.4 $\pm$ 5.9 (14%)	267 $\pm$ 29 (4%)
2	12.1 $\pm$ 0.7 (83%)	51.7 $\pm$ 7.4 (12%)	225 $\pm$ 21 (5%)
3	11.4 $\pm$ 0.6 (83%)	56.3 $\pm$ 6.6 (11%)	229 $\pm$ 20 (6%)
4	10.2 $\pm$ 0.6 (83%)	49.6 $\pm$ 7.4 (10%)	190 $\pm$ 13 (7%)
6	9.4 $\pm$ 0.4 (83%)	51.8 $\pm$ 6.1 (10%)	199 $\pm$ 12 (7%)
8	9.2 $\pm$ 0.5 (81%)	51.9 $\pm$ 6.1 (11%)	200 $\pm$ 12 (8%)

decay time constants,  $\tau_1$ ,  $\tau_2$  and  $\tau_3$ . The obtained decay time constants for scintillator mixtures with the different concentrations of NOL 37 are represented in Table 1. The values in the brackets are the contributions of the components to the total light yield. It should be noted that the contribution of the fastest component is more than 80% of the total light yield. The emission kinetics of LAB + 1.5 g/L PPO is characterized by decay time constants  $\tau_1 = 6.8 \pm 0.5$  ns (59%),  $\tau_2 = 16.3 \pm 0.8$  ns (37%) and  $\tau_3 = 64 \pm 4$  ns (4%).

#### 4 Light yield and emission kinetics stability of LAB-based scintillators with NOL 37 fluor

Modern large-scale experiments in astroparticle and neutrino physics are designed to run for many years of operation, typically 10 years or more. Therefore, the long-term stability of the scintillator is one of the most important parameters. To perform long-term measurements for new developments is a difficult task. However, the stability of the light yield and the emission kinetics for four full years from June 2018 to June 2022 has been measured. EJ204 plastic scintillator of 2 cm in diameter and 1 cm thick was chosen as a reference scintillator,

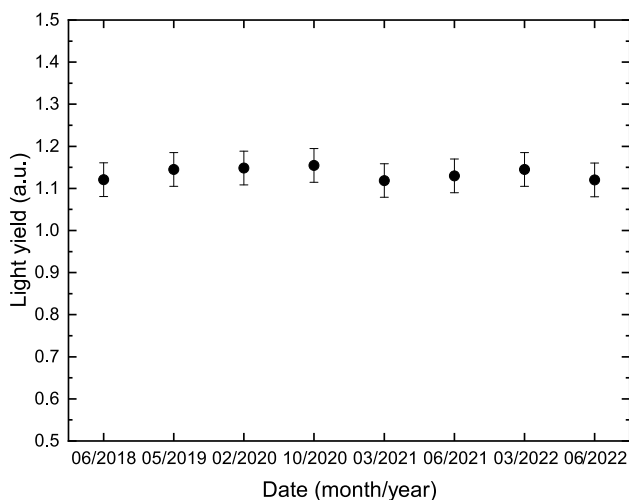


**Fig. 7** Light yield of the developed LAB-based scintillator with NOL 37 kept stable between June 2018 and June 2022

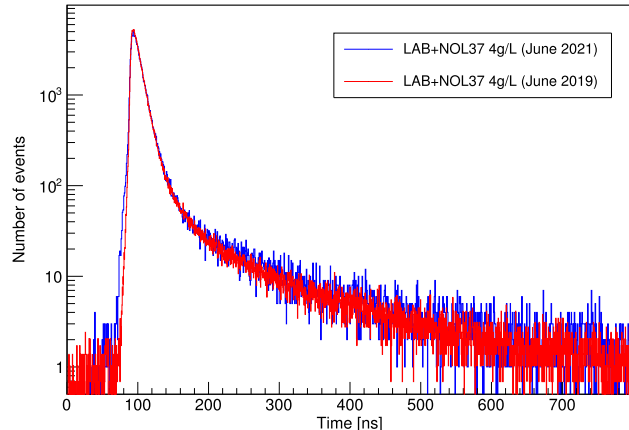


**Fig. 8** Light emission kinetics of LAB-based scintillator with NOL 37 measured in June 2019 (red colour) and June 2021 (blue colour)

relative to which the light yield has been measured. The light yield stability of the EJ204 and the PMT's sensitivity were monitored by the average number of photoelectrons in the PMT when the scintillator was irradiated with alpha-particles from the  $^{241}\text{Am}$  radioactive source. The PMT's sensitivity has been controlled throughout the measurements using a calibrated radio-luminescent source (RLS) [11] coupled to the PMT's window by counting single-photoelectron pulses.

The measurement results of the light yield stability of the developed LAB-based scintillator with NOL 37 are shown in Fig. 7. The emission kinetics stability of the developed liquid scintillator was also studied. Figure 8 shows the emission kinetics spectra measured in June 2019 and June 2021.

As can be seen from Figs. 7 and 8, no changes in the light yield and the emission kinetics of the developed liquid scintillator were found over three years of measurements.

#### 5 Conclusion

We developed new organosilicon fluor and LAB-based liquid scintillator with such fluor. The advantage of the liquid scintillator with new fluor is its high light yield, almost two times higher than the light yield of the scintillator with PPO. It should be noted that the liquid scintillator with the new

fluor has a slightly slower light emission kinetics in comparison with scintillators with PPO. The measurement results of newly developed scintillator represent an intermediate step of an ongoing development programme. It is expected that further optimization of the composition of new organosilicon fluors will improve further the scintillation properties of liquid scintillators. Studies of the new organosilicon fluors show very promising results and we believe that the new fluors will be successfully applied in the next-generation large-scale experiments in neutrino and astroparticle physics.

**Acknowledgements** This work is supported by the Ministry of science and higher education of the Russian Federation under the contract No-075-15-2020-778 in the framework of the Large scientific projects program within the national project “Science”.

**Data Availability Statement** This manuscript has no associated data or the data will not be deposited. [Authors’ comment: The data will be available at any time by contacting the corresponding author.]

**Open Access** This article is licensed under a Creative Commons Attribution 4.0 International License, which permits use, sharing, adaptation, distribution and reproduction in any medium or format, as long as you give appropriate credit to the original author(s) and the source, provide a link to the Creative Commons licence, and indicate if changes were made. The images or other third party material in this article are included in the article’s Creative Commons licence, unless indicated otherwise in a credit line to the material. If material is not included in the article’s Creative Commons licence and your intended use is not permitted by statutory regulation or exceeds the permitted use, you will need to obtain permission directly from the copyright holder. To view a copy of this licence, visit <http://creativecommons.org/licenses/by/4.0/>.

Funded by SCOAP<sup>3</sup>. SCOAP<sup>3</sup> supports the goals of the International Year of Basic Sciences for Sustainable Development.

## References

1. A. Gando et al., Reactor on-off antineutrino measurement with KamLAND. *Phys. Rev. D* **88**, 033001 (2013). <https://doi.org/10.1103/PhysRevD.88.033001>
2. G. Bellini et al., Precision measurement of the  ${}^7\text{Be}$  solar neutrino interaction rate in Borexino. *Phys. Rev. Lett.* **107**, 141302 (2011). <https://doi.org/10.1103/PhysRevLett.107.141302>
3. F.P. An et al., Measurement of electron antineutrino oscillation based on 1230 days of operation of the Daya Bay experiment. *Phys. Rev. D* **95**, 072006 (2017). <https://doi.org/10.1103/PhysRevD.95.072006>
4. S.H. Seo et al., Spectral measurement of the electron antineutrino oscillation amplitude and frequency using 500 live days of RENO data. *Phys. Rev. D* **98**, 012002 (2018). <https://doi.org/10.1103/PhysRevD.98.012002>
5. Y. Abe et al., Improved measurements of the neutrino mixing angle  $\theta_{13}$  with the Double Chooz detector. *JHEP* **10**, 086 (2014) (Erratum: *JHEP* 02, 074 (2015)). [https://doi.org/10.1007/JHEP02\(2015\)074](https://doi.org/10.1007/JHEP02(2015)074). [arXiv:1406.7763](https://arxiv.org/abs/1406.7763) [hep-ex]
6. T. Adam et al., JUNO Conceptual Design Report (2015). [arXiv:1508.07166](https://arxiv.org/abs/1508.07166) [physics.ins-det]
7. F.P. An et al., The detector system of the Daya bay reactor neutrino experiment. *Nucl. Instrum. Methods A* **811**, 133–161 (2016). <https://doi.org/10.1016/j.nima.2015.11.144>. [arXiv:1508.03943](https://arxiv.org/abs/1508.03943) [physics.ins-det]
8. J.S. Park et al., Production and optical properties of Gd-loaded liquid scintillator for the RENO neutrino detector. *Nucl. Instrum. Methods A* **707**, 45–53 (2013). <https://doi.org/10.1016/j.nima.2012.12.121>
9. S. Lubsandorzhiev et al., Development of new liquid scintillators for neutrino experiments of next generation. *Proc. Sci.* **358** (2019)
10. W. Becker, *Advanced Time-Correlated Single Photon Counting Techniques* (Springer, Berlin, 2005)
11. G.A. Mikhachenko, *Radioluminescent Emitters* (Energoatomizdat, Moscow, 1988)